Journal of Materials Chemistry A

Accepted Manuscript

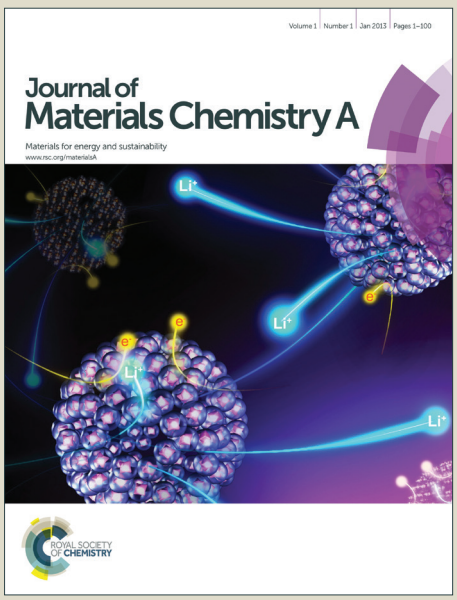

ROYAL SOCIETY OF CHEMISTRY

www.rsc.org/materialsA

Journal Name

ARTICLE

Photocatalytic reduction of CO_2 with water promoted by Ag clusters in Ag/Ga_2O_3 photocatalyst†

Received 00th January 20xx,
Accepted 00th January 20xx

DOI: 10.1039/x0xx00000x

www.rsc.org/

Muneaki Yamamoto,*[a] Tomoko Yoshida,*[b,c] Naoto Yamamoto,[a] Toyokazu Nomoto,[d] Yuta Yamamoto,[c] Shinya Yagi[c] and Hisao Yoshida[e,f]

Ag loaded Ga_2O_3 (Ag/Ga_2O_3) photocatalysts were prepared by an impregnation method, and examined for photocatalytic reduction of CO_2 with water where CO, H_2 and O_2 were formed as products. TEM and X-ray absorption near edge structure (XANES) measurements revealed that around 1 nm sized Ag clusters were formed predominantly in an active Ag/Ga_2O_3 sample while partially oxidized large Ag particles with the size of several – several tens nm were observed in a less active Ag/Ga_2O_3 samples. Both Ag L_3-edge and O K-edge XANES analysis suggested that the small Ag clusters accepted more electrons in the *d*-orbitals as the result of the strong interaction with the Ga_2O_3 surface. In-situ FT-IR measurements for the Ag/Ga_2O_3 samples showed CO_3 stretching vibration bands assignable to monodentate bicarbonate and bidentate carbonate species chemisorbed on the Ga_2O_3 surface, and to monodentate carbonate species on the large Ag particles. Among these chemisorbed species, the monodentate bicarbonate and/or the bidentate carbonate species changed to bidentate formate species, as the reaction intermediate, under the UV light irradiation. The bidentate formate species was formed not by the plasmonic excitation of the Ag nanoparticles but by the photoexcitation of the Ga_2O_3 semiconductor, and the formation process would be promoted at the perimeter of the Ag clusters on the Ga_2O_3 surface by the effective separation of electron-holes pairs.

Introduction

Photocatalytic CO_2 reduction with water to usable products has attracted much attention because of its potential to realize an artificial photosynthesis.[1,2] To use water as a reductant for CO_2 reduction, the activation of water is intrinsically required. Thus, heterogeneous metal oxide photocatalysts which can activate water have been widely studied toward CO_2 reduction with water. Recently, it has been reported that both the photocatalytic activity and selectivity for CO_2 reduction to CO is improved by loading of Ag as a cocatalyst on several metal oxide photocatalysts such as $BaLa_4Ti_4O_{15}$,[3] Ga_2O_3,[4] Zn-doped Ga_2O_3,[5] $ZnGa_2O_4$,[6] $KCaSrTa_5O_{15}$,[7,8] $CaTiO_3$,[9] $La_2Ti_2O_7$,[10] and SrO-modified Ta_2O_5.[11]

The Ag cocatalyst has been considered as one of the effective electron receiving sites to promote the separation of photogenarated electron-hole pairs as well as the possible CO_2 reduction sites to produce CO.[3-11] It has been also proposed that the particle size and chemical state of the Ag should affect the photocatalytic activity, and metallic Ag nanoparticles with the small size and uniform distribution contribute to the enhancement for the photocatalytic conversion of CO_2 with water.[3,6,11]

In our previous study, Ga_2O_3 which is known as an active photocatalyst for water splitting[12] promoted photocatalytic reduction of CO_2 with water and the photocatalytic activity was enhanced by loading of Ag.[4,13] We have carried out in-situ FT-IR measurements of Ag loaded Ga_2O_3 (Ag/Ga_2O_3) photocatalysts at each reaction steps, and proposed the reaction mechanism involving the generation process of bidentate formate species as the reaction intermediates.[14]

In the present study, we focused on the influence of the structural and chemical states of Ag catalyst as well as its interaction with Ga_2O_3 support on the reaction mechanism for the photocatalytic reduction of CO_2 with water over Ag/Ga_2O_3. The size of the Ag particles was investigated by TEM measurements. Diffuse reflectance UV-visible spectra was carried out to obtain information of the size and chemical state of the Ag cocatalyst. In order to clarify the surface chemical state of Ag/Ga_2O_3 samples, we measured Ag L_3-edge and O K-edge X-ray absorption near edge structure (XANES) spectra of the samples. In situ FT-IR spectroscopy was applied to Ag/Ga_2O_3 samples to understand the reaction steps such as the adsorption of CO_2 molecules, and the subsequent generation of bidentate formate species as the reaction intermediates. Through these analyses, the function of the Ag cocatalyst was discussed.

Experimental

[a] *Graduate School of Engineering, Nagoya University, Nagoya 464-8603, Japan. Email: yamamoto.muneaki@f.mbox.nagoya-u.ac.jp*
[b] *Advanced Research Institute for Natural Science and Technology, Osaka City University, Osaka 558-8585, Japan. Email: tyoshida@ocarina.osaka-cu.ac.jp*
[c] *EcoTopia Science Institute, Nagoya University, Nagoya 464-8603, Japan*
[d] *Aichi Synchrotron Radiation Center, Seto 489-0965, Japan*
[e] *Graduate school of human and environmental studies, Kyoto University, Kyoto 606-8501, Japan*
[f] *Element Strategy Initiative for Catalysts and Batteries (ESICB), Kyoto University, Kyoto 615-8520, Japan*
† Electronic Supplementary Information (ESI) available. See DOI: 10.1039/x0xx00000x

Catalysts preparation.

Ag/Ga_2O_3 samples were prepared by an impregnation method. A mixture of a Ga_2O_3 powder (Kojundo Chemical Laboratory Co. Ltd. purity 99.99 %) and an aqueous solution of $AgNO_3$ (Kishida Chemical Co. Ltd. purity 99.8 %) was magnetically stirred and dried up, followed by calcination at 673 K for 2 h, which provided the Ag/Ga_2O_3 samples. The loading amounts of Ag were 0.1, 0.2, 0.5 and 1.0 wt%.

Reaction tests.

The photocatalytic reaction tests were conducted in a specially designed reactor of gas–liquid–solid three phases as follows: Before the reaction test, the Ag/Ga_2O_3 powder (0.2 g) in the reactor was irradiated from a 300 W Xe lamp for 1 h under CO_2 gas with a flow rate at 3.0 mL/min, where the light intensity measured in the range of 254 ± 10 nm was 25 mW/cm^2. Then a $NaHCO_3$ aqueous solution (H_2O 10 mL, $NaHCO_3$ 0.92 g) was added to this reactor cell in dark. After 1 h, the background was measured with an online gas chromatograph with thermal conductivity detector (GC-TCD, Shimadzu GC-8APT). Successively, photocatalytic reduction of CO_2 under photoirradiation was started and CO, H_2 and O_2 production rates were measured every 1 h with the GC-TCD up to five repetitions.

TEM measurements.

For TEM measurements, samples were dispersed in an ethanol solution, and a drop of the suspension was mounted on a holey carbon covered copper mesh. TEM images of samples were recorded with a Hitachi H-800 electron microscope operated at 200 kV at the High Voltage Electron Microscope Laboratory in Nagoya University.

Cs-corrected S/TEM (JEOL, JEM-ARM 200F Cold) equipped with a thermal field-emission gun was operated at 200 kV. HAADF-STEM images were taken at almost just focus at a resolution of 1024 × 1024 pixels (0.021 × 0.021 nm^2 pixel^{-1}).

DR UV-Vis spectroscopy.

Diffuse reflectance UV–visible spectrum was recorded at room temperature on a spectrophotometer (JASCO V-670) equipped with an integrating sphere covered with $BaSO_4$, where $BaSO_4$ was used as the reference.

XANES spectroscopy.

XANES measurements were carried out at the beam line 6N1 and 7U at Aichi Synchrotron Radiation Center. Ag L_3-edge XANES spectra of the samples were measured using a two-crystal Ge(111) monochromator at room temperature in an atmospheric chamber with He gas. The data were recorded in a fluorescent X-ray yield mode with a silicon drift detector (Vortex Electronics). O K-edge XANES spectra of the samples were measured at room temperature in a total electron yield mode, where the X-ray energy dependence of the O Auger electron yield was monitored. Considering the escape depth of the Auger electrons, the spectra showed the state of the surface layers up to a few nm in depth.[15]

FT-IR spectroscopy.

FT-IR spectra were recorded with a FT/IR-6100 (JASCO) in a transmission mode at room temperature. Sample (ca.15 mg) was pressed into a disk (diameter: 10 mm) at 50 MPa and placed in an in-situ IR cell equipped with CaF_2 windows. The cell allowed us to perform heating, introduction of substrates, photoirradiation, and measurement of spectra in-situ. Before the measurement, the sample was evacuated at 673 K for 1h. For each spectrum, the data from 6 scans were accumulated at a resolution of 4 cm^{-1}.

Results and discussion

Photocatalytic reduction of CO_2 with water over the Ag/Ga_2O_3 samples.

The prepared Ag/Ga_2O_3 samples were examined for the photocatalytic reduction of CO_2 with water. Table 1 shows photocatalytic activity for the reaction over a bare Ga_2O_3 sample, the 0.1 wt% Ag/Ga_2O_3 sample and the 1.0 wt% Ag/Ga_2O_3 sample after 5 h. The products observed in the present study were CO, H_2 and O_2, which consisted with the results in other reports.[3-11,13,14] In the present system, both the CO_2 reduction and water splitting would take place competitively. The CO production rates over all the Ag/Ga_2O_3 samples were faster than that over the bare Ga_2O_3 sample. It was confirmed that the Ag cocatalyst well accelerated the CO production. The CO production rate over the 0.1 wt% Ag/Ga_2O_3 sample was faster than that over the 1.0 wt% Ag/Ga_2O_3 sample, while the selectivity to CO was higher for the latter sample. These results should derive from the difference in the structural and chemical state of the Ag cocatalyst among these samples.

Ag species in Ag/Ga_2O_3 samples.

Figure 1 shows TEM images of the Ag/Ga_2O_3 samples. The size distribution of the Ag particles varied with the loading amount of Ag. The Ag particles with the size of several tens nm were observed in the 0.1 wt% Ag/Ga_2O_3 sample, but the number of particles was very few and a smaller particle was not found. On the other hand, the Ag particles with the size of several–several tens nm were observed in the 1.0 wt% Ag/Ga_2O_3 sample. Note that many Ag particles with the size of several nm existed in the 1.0 wt% Ag/Ga_2O_3 sample. The size of several nm was smaller than that of Ag particles observed in the 0.1 wt% Ag/Ga_2O_3 sample although the larger amount of Ag loading might provide the larger Ag particle. Considering the resolution of TEM measurement, this result probably indicates the presence of ca. 1 nm or sub nm sized Ag particles in the 0.1 wt% Ag/Ga_2O_3 sample.

To confirm the existence of such very small Ag particles, we conducted the HR-STEM measurement for the 0.1 wt% Ag/Ga_2O_3 sample. HR-STEM successfully revealed the presence of the small Ag particles in the 0.1 wt% Ag/Ga_2O_3 sample as indicated by the arrows in Figure 2a, which size was estimated around 1 nm in diameter. Figure 2b shows the distribution of the particle size estimated from more than twenty images, where the majority was found around 1 nm.

Figure 3 gives a diffuse reflectance UV-visible spectrum of the 0.1 wt% Ag/Ga_2O_3 sample. A large absorption band for bandgap excitation of Ga_2O_3 was observed less than 300 nm in wavelength. No clear band assignable to a localized surface plasmon resonance of

Ag nanoparticles around 450 nm was observed, while a very small band at 350 nm due to Ag small clusters (Ag_n)[16] was found. This is consistent with the result obtained by the TEM and HR-STEM measurements.

Figure 4 shows the Ag L_3-edge XANES spectra of the Ag/Ga_2O_3 samples together with those of Ag foil and Ag_2O reference samples. Ag L_3-edge XANES arises mainly from the excitation of the $2p_{3/2}$ core level electron into the unoccupied states of d character above the Fermi level. The XANES spectrum of the 1.0 wt% Ag/Ga_2O_3 sample exhibited a sharp absorption (whiteline) at 3353 eV due to the oxidized Ag as well as the fine resonance peaks around 3380 and 3400 eV characteristic of the metallic Ag. However, this spectrum could not be reproduced by simple imposing the spectra of the Ag foil and the Ag_2O reference samples. This result suggests that Ag metal particles in the 1.0 wt% Ag/Ga_2O_3 sample would be not a mixture of large metallic particles and large oxidized particles but probably partially oxidized large particles. Note that the absorption features due to the Ag metal and oxides in the spectra of the Ag/Ga_2O_3 samples became weaker with decreasing the loading amount of Ag, and indistinct broad feature was observed. As mentioned in Supporting Information with Figure S1† and S2†, it was confirmed that the broad peaks were not due to the decreased amount of Ag but to the decreased Ag particle size and/or the enhanced interaction between the Ag clusters and the Ga_2O_3 surface. It is thus suggested that the Ag species in the 0.1 wt% Ag/Ga_2O_3 sample would be well dispersed to form Ag clusters, as a result which would be strongly interacted with the Ga_2O_3 surface. This should support the explanation mentioned above for the TEM and HR-STEM images and DR UV-Vis spectrum, i.e., the Ag clusters with the size of around 1 nm were mainly present in the 0.1 wt% Ag/Ga_2O_3 sample. If there were large particles with the size of several tens nm in this sample mainly, its XANES spectrum should be more similar to that of the Ag foil. Thus, the large particles observed in the TEM image would be minor in this sample.

We investigated the difference in the chemical state of the Ag species among the above two samples in detail. It is expected that the chemical states of the Ag species would change with heating atmosphere. Figure 5 illustrates the Ag L_3-edge XANES spectra of the samples heated at 673 K for 2 h in air or in vacuum. As for the 1.0 wt% Ag/Ga_2O_3 sample, the significant effect of heating atmosphere was found on the XANES feature. The XANES spectrum of the sample heated in vacuum was substantially similar to that of the Ag foil, although a shoulder at 3353 eV was still observed. By heating up to 673 K in vacuum, the partially oxidized large Ag particles as prepared were almost decomposed to Ag metal particles. On the other hand, the XANES spectrum of the 0.1 wt% Ag/Ga_2O_3 sample heated in vacuum was almost the same as that of the sample heated in air. This result indicates that the well dispersed Ag particles, i.e. the Ag clusters, in the 0.1 wt% Ag/Ga_2O_3 sample would be stable even under the heating. The stability should be attributed to the strong interaction between the Ag cluster and the Ga_2O_3 surface.

Actually, in Figure 6, the characteristic XANES feature just above the edge would represent the interaction between the Ag cluster and the Ga_2O_3 surface. The absorption band just above the edge around 3350–3365 eV is lower for the Ag/Ga_2O_3 samples rather than a bulk Ag metal, which was most significant for the 0.1 wt% Ag/Ga_2O_3 sample. Similar features were reported by Bzowski *et al*. for the XANES spectra of Au-Ag alloys and they concluded that the electron density in the *d*-orbital of the Ag atom increased by alloying with Au.[17] Therefore, in the present Ag/Ga_2O_3 samples, the Ag species would probably accept more electrons in the *d*-orbitals as the result of interaction with the Ga_2O_3 surface, in other words, the electron density in the *d*-orbitals of the Ag atom would be increased by the hybridization with the band of the Ga_2O_3 surface. This phenomenon seemed more significant for the 0.1 wt% Ag/Ga_2O_3 sample. Thus, the Ag cluster in the 0.1 wt% Ag/Ga_2O_3 sample would interact with the Ga_2O_3 surface stronger than the partially oxidized large Ag particles in the 1.0 wt% Ag/Ga_2O_3 sample.

The interaction of the Ag–Ga_2O_3 interface was also discussed based on the O K-edge XANES involving the excitation of O 1s core level to the unoccupied 2p states. The spectra were recorded by the total electron yield mode and thus the obtained information would reflect only the state of the surface layers by considering the electron escape depth. Figure 7 shows the O K-edge XANES spectra of the Ag/Ga_2O_3 samples and the bare Ga_2O_3 sample which have been stored in an air atmosphere and evacuated at room temperature. The shoulder at 531.5 eV assigned to the absorption of silver oxides species[18] grew with an increase of the Ag loading, suggesting that the partially oxidized Ag particles would exist preferentially on the Ag/Ga_2O_3 samples with higher Ag loading. Two broad peaks observed around 534.5 eV and 540.5 eV could be attributed to the excitation of O 1s to hybridized orbital of the metal sp and O 2p orbitals.[18-21] Note that the peak at 534.5 eV was higher for the 0.1 wt% Ag/Ga_2O_3 sample rather than the bare Ga_2O_3, implying that the unoccupied O 2p orbital of the Ga_2O_3 surface was increased by the interaction of the Ag–Ga_2O_3 interface. This should not be due to the increase of the amount of the silver oxides species in the samples, since the intensity of this peak decreased for the samples containing more silver oxide species such as the 1.0 wt% Ag/Ga_2O_3 sample. These results correspond to that obtained by the Ag L_3-edge XANES spectra and indicate the electron donation to some extent from the O atoms of the Ga_2O_3 surface to the Ag atoms in the Ag clusters. Thus, Ag L_3- and O K-edge XANES spectra demonstrated that the interaction between the Ag species and the Ga_2O_3 surface influences the electronic states of them, which would be more significant for the small size of the Ag clusters such as 1 nm. It is known that the work function of a smaller metal particle is larger than that of a large particle,[22] in other words, the fermi level of the Ag clusters would be lower. This causes more electron donation from the n-type semiconductor Ga_2O_3 to the Ag metal through the metal-semiconductor junction. Therefore, the *d*-orbital of the Ag cluster would be more filled.

As a conclusion of this section, TEM images, DR UV-Vis and XANES spectra clarified the followings: In the Ag/Ga_2O_3 sample with the small amount of Ag loading, Ag clusters with the size of around 1 nm were formed predominantly. They had strong interaction with Ga_2O_3 supports, which caused the electron donation to some extent from the O atoms of the Ga_2O_3 surface to the Ag atoms in the Ag clusters. On the other hand, in the Ag/Ga_2O_3 sample with the large amount of Ag loading, partially oxidized large Ag particles existed and they were likely to decompose to metallic Ag particles with the heat treatment in vacuum. These differences in the size and chemical state of Ag species would affect not only the

photocatalytic activity for the CO_2 reduction with water but also the reaction mechanism.

Functions of the Ag cluster.

Here, we carried out in-situ FT-IR measurements of the Ag/Ga_2O_3 samples at each reaction steps. In this paper, the difference IR spectrum of a sample was obtained by subtracting the background spectrum of the sample after the heat treatment in vacuum. Therefore, the partially oxidized large Ag particles became metallic before the measurements. Figure 8 shows the difference FT-IR spectra of the adsorbed species on the Ag/Ga_2O_3 samples after introduction of 45 Torr of CO_2. The bands at 1635 and 1420 cm^{-1} are assigned to asymmetric CO_3 stretching vibration [$\nu_{as}(CO_3)$] and symmetric CO_3 stretching vibration [$\nu_s(CO_3)$] of monodentate bicarbonate species, respectively.[23-26] The bands at 1590 and 1320 cm^{-1} are ascribed to $\nu_{as}(CO_3)$ and $\nu_s(CO_3)$ of bidentate carbonate species, respectively.[23-25] These bands were observed in all of the spectra regardless of the loading amount of Ag. CO_2 molecules would react with the surface hydroxy group and the surface lattice oxygen of Ga_2O_3 to form the bicarbonate and carbonate species, respectively.[27,28] On the other hand, the bands around 1510 and 1350 cm^{-1} are assigned to $\nu_{as}(CO_3)$ and $\nu_s(CO_3)$ of monodentate carbonate species, respectively,[23,29-31] and these bands increased with the loading amount of Ag. Since the formation of the CO_3 species from CO_2 molecule are expected to require the surface oxygen,[29,32] the large Ag metal particles would be covered with a surface oxide layer even after the heat treatment, and the monodentate carbonate species would be formed on them.

Figure 9 illustrates the difference FT-IR spectra of the samples after introduction of CO_2, followed by evacuation and photoirradiation for 1 h. The bands derived from the carbonate and bicarbonate species decreased and new bands appeared at 1577, 1388 and 1353 cm^{-1}. These bands are assigned to $\nu_{as}(CO_2)$, $\delta(CH)$ and $\nu_s(CO_2)$ of bidentate formate species, respectively.[24-26] The intensity of the bands ascribed to the bidentate formate species was high for the Ag/Ga_2O_3 samples with smaller amount of Ag loading such as the 0.1 wt% Ag/Ga_2O_3 sample, while low for the 1.0 wt% Ag/Ga_2O_3 sample. This result indicates that the bidentate formate species would arise from not the monodentate carbonate species adsorbed on the large Ag metal particles but the monodentate bicarbonate and/or the bidentate carbonate adsorbed on the Ga_2O_3 surface. We had also conducted in-situ FT-IR measurements using the visible light which could not excite electrons of Ga_2O_3 but of plasmonic Ag nanoparticles, and confirmed no reaction proceeded. This result suggests that the bidentate formate species was formed not by the plasmonic excitation of the Ag nanoparticles but by the electron excitation of the Ga_2O_3 semiconductor.

On the basis of these FT-IR results and our previous study,[14] we propose tentative reaction schemes for the photocatalytic reduction of CO_2 with water over 0.1 wt% Ag/Ga_2O_3 sample as shown in Figure S3†. Since the formation of the bidentate formate species was promoted by the Ag clusters included in the 0.1 wt% sample, the Ag clusters would be one of the photocatalytic active sites that could form carbon monoxide via the bidentate formate species. As mentioned, Ag metal particle generally shows an increase of its work function when the particles size is reduced,[22] therefore, such small Ag clusters could more enhance the band bending at the metal-semiconductor junction, promoting the separation of photoexcited electron and hole pairs. As a result, the Ag cluster would effectively reduce the monodentate bicarbonate and/or the bidentate carbonate to produce the bidentate formate intermediate species. The adsorbed CO_2 species would migrate on the surface to the perimeter of the Ag clusters in turn to be reduced.

On the other hand, the large Ag metal particles in the 1.0 wt% Ag/Ga_2O_3 sample would have a capacity to trap many photoexcited electrons, and the Ag clusters, even if existence, could receive less electron competitively. Thus, the large Ag metal particles might prevent from producing the bidentate formate species at the perimeters of the Ag clusters. If the trapped electrons by the large Ag metal particles were provided for CO_2 reduction, they would be used for the reduction of monodentate carbonate species.

On the 1.0 wt% Ag/Ga_2O_3 sample, the bidentate formate species was not observed although a certain amount of carbon monoxide was formed. At present, although the reaction on the large metal Ag particles has not been clarified yet, we might point out some possibilities: One is that, if the bidentate formate species was produced, the further reaction might be too fast to detect them in the present FT-IR measurement.[31] Another is that, if the bidentate formate species was not formed, the monodentate carbonate generated on the large Ag metal particles might rather be converted to carbon monoxide. Further study is required.

Conclusions

In the photocatalytic reduction of CO_2 with water with the Ag loaded Ga_2O_3 photocatalysts, the CO production rate depended on the loading amount of Ag and the 0.1 wt% Ag/Ga_2O_3 sample showed higher CO production rate than the 1.0 wt% Ag/Ga_2O_3 sample. We investigated the structural and chemical states of the Ag cocatalyst as well as its interaction with the Ga_2O_3 surface by measuring TEM images, DR UV-Vis and XANES spectra.

In the Ag/Ga_2O_3 samples with low Ag loading, around 1 nm sized Ag clusters were formed predominantly. Such dispersed Ag clusters had strong interaction with the Ga_2O_3 surface, which caused the electron donation to some extent from the O atoms of the Ga_2O_3 surface to the Ag atoms in the Ag clusters. With an increase of Ag loading, additional Ag particles with the size of several – several tens nm increased. These large particles were partially oxidized, and likely to decompose to Ag metal ones when it was heated in vacuum.

In addition, we have carried out in-situ FT-IR measurements of the Ag/Ga_2O_3 photocatalysts at each reaction steps, and revealed the following CO_2 adsorption behaviours: CO_2 molecules mainly adsorbed on the Ga_2O_3 surface to form the monodentate bicarbonate and the bidentate carbonate species. And the small Ag clusters on the Ga_2O_3 surface would not have a significant influence on the amounts of these adsorbed species. On the other hand, CO_2 molecules adsorbed on the large Ag metal particles to form monodentate carbonate species. The bidentate formate species as the reaction intermediate was generated from not the monodentate carbonate species on the large Ag metal particles but the monodentate bicarbonate and/or the bidentate carbonate species on the Ga_2O_3 surface. The formation of the bidentate formate species would take place at the perimeters of the Ag clusters on the Ga_2O_3 surface, because such small Ag clusters could enhance the band bending in

the Ga_2O_3 semiconductor, promoting the effective separation of the photoexcited electrons and holes.

Acknowledgements

This work was supported by a Grant-in-Aid for Scientific Research (No.24360332 and 24656489) from the Japan Society for the Promotion of Science (JSPS). Synchrotron experiments were carried out at Aichi Synchrotron Radiation Center which is supported by No.2503042.

References

1 A. Kubacka, M. Fernández-García and G. Colón, *Chem. Rev.*, 2012, **112**, 1555.
2 D. Chen, X. Zhang and A. F. Lee, *J. Mater. Chem. A*, 2015, DOI: 10.1039/c5ta01592h.
3 K. Iizuka, T. Wato, Y. Miseki, K. Saito and A. Kudo, *J. Am. Chem. Soc*., 2011, **133**, 20863.
4 Z. Like, E. Tanabe, K. Morikawa, T. Kazino, T. Sekihuzi, S. Matumoto, Y. Hirata and H. Yoshida, *108th Symposium of Catal. Soc. A*, 2011, 1D15 (in Japanese).
5 K. Teramura, Z. Wang, S. Hosokawa, Y. Sakata and T. Tanaka, *Chem. Eur. J*., 2014, **20**, 9906.
6 Z. Wang, K. Teramura, S. Hosokawa and T. Tanaka, *J. Mater. Chem. A*, 2015, **3**, 11313.
7 T. Takayama, K. Tanabe, K. Saito, A. Iwase and A. Kudo, *Phys. Chem. Chem. Phys*., 2014, **16**, 24417.
8 T. Takayama, A. Iwase and A. Kudo, *Bull. Chem. Soc. Jpn*., 2015, **88**, 538.
9 H. Yoshida, L. Zhang, M. Sato, T. Morikawa, T. Kajino, T. Sekito, S. Matsumoto and H. Hirata, *Catal. Today*, 2015, **251**, 132.
10 Z. Wang, K. Teramura, S. Hosokawa and T. Tanaka, *Appl. Catal. B: Environ.*, 2015, **163**, 241.
11 K. Teramura, H. Tatsumi, Z. Wang, S. Hosokawa and T. Tanaka, *Bull. Chem. Soc. Jpn*., 2015, **88**, 431.
12 T. Yanagida, Y. Sakata and H. Imamura, *Chem. Lett*., 2004, **33**, 726.
13 N. Yamamoto, T. Yoshida, S. Yagi, Z. Like, T. Mizutani, S. Ogawa, H. Nameki and H.Yoshida, *e-J. Surf. Sci. Nanotech*., 2014, **12**, 263.
14 M. Yamamoto, T. Yoshida, N. Yamamoto, H. Yoshida and S. Yagi, *e-J. Surf. Sci. Nanotech*., 2014, **12**, 299.
15 A. Erbil, G. S. Cargil, R. Frahm and R. F. Boehme, *Phys. Rev. B*, 1988, **37**, 2450.
16 A. N. Pestryakov and A. A. Davydov, *J. Electron Spectrosc. Relat. Phenom.*, 1995, **74**, 195.
17 A. Bzowski, Y. M. Yiu and T. K. Sham, *Jpn. J. Appl. Phys*., 1993, **32**, 691.
18 V. I. Bukhtiyarov, M. Havecker, V. V. Kaichev, A. Knop-Gericke, R. W. Mayer and R. Schlogl, *Phys. Rev. B*, 2003, **67**, 235422.
19 F. Tourtin, P. Armand, A. Ibanez, G. Tourillon and E. Philippot, *Thin Solid Films*, 1998, **322**, 85.
20 W-S. Yoon, K-B. Kim, M-G. Kim, M-K. Lee, H-J. Shin, J-M. Lee, J-S. Lee and C-H. Yo, *J. Phys. Chem. B*, 2002, **106**, 2526.
21 X. T. Zhou, F. Heigl, J. Y. P. Ko, M. W. Murphy, J. G. Zhou, T. Regier, R. I. R. Blyth and T. K. Sham, *Phys. Rev. B*, 2007, **75**, 125303.
22 D. M. Wood, *Phys. Rev. Lett.*, 1981, **46**, 749.
23 G. Busca and V. Lorenzelli, *Mater. Chem*., 1982, **7**, 89-126.
24 S. E. Collins, M. A. Baltanas and A. L. Bonivardi, *J. Catal*., 2004, **226**, 410.
25 S. E. Collins, M. A. Baltanas and A. L. Bonivardi, *J. Phys. Chem. B*, 2006, **110**, 5498.
26 H. Tsuneoka, K. Teramura, T. Shishido and T. Tanaka, *J. Phys. Chem. C,* 2010, **114**, 8892.
27 M. Primet, P. Pichat and M.-V. Mathieu, *J. Phys. Chem*., 1971, **75**, 1221.
28 S. Neatu, J. A. Macia-Agullo, P. Concepcion and H. Garcia, *J. Am. Chem. Soc*., 2014, **136**, 15969.
29 E. M. Stuve, R. J. Madix and B. A. Sexton, *Chem. Phys. Lett*., 1982, **89**, 48.
30 J. I. D. Cosimo, V. K. Díez, M. Xu, E. Iglesia and C. R. Apesteguía, *J. Catal*., 1998, **178**, 499.
31 M. F. Baruch, J. E. Pander III, J. L. White and A. B. Bocarsly, *ACS Catal*. 2015, **5**, 3148.
32 C. T. Campbell and M. T. Paffett, *Surf. Sci*., 1984, **143**, 517.

Table 1. Results of photocatalytic reduction of CO_2 with water over a bare Ga_2O_3 and Ag/Ga_2O_3 samples after 5 h.

photocatalyst	CO production rate (μmol/h)	H_2 production rate (μmol/h)	O_2 production rate (μmol/h)
Ga_2O_3	0.4	2.4	0.6
0.1 wt% Ag/Ga_2O_3	2.0	9.4	4.6
1.0 wt% Ag/Ga_2O_3	1.1	0.7	—

Figure Captions

Figure 1. TEM images of 0.1 wt% Ag/Ga_2O_3 (a) and 1.0 wt% Ag/Ga_2O_3 (b).

Figure 2. HAADF-STEM image of 0.1 wt% Ag/Ga_2O_3 (a) and the size distribution of Ag particles (b).

Figure 3. Diffuse reflectance UV-Vis absorption spectrum of 0.1 wt% Ag/Ga_2O_3.

Figure 4. Ag L_3-edge XANES spectra of 0.1 wt% Ag/Ga_2O_3 (a), 0.2 wt% Ag/Ga_2O_3 (b), 0.5 wt% Ag/Ga_2O_3 (c), 1.0 wt% Ag/Ga_2O_3 (d) and Ag references.

Figure 5. Ag L_3-edge XANES spectra of 0.1 wt% Ag/Ga_2O_3 heated at 673 K in air (a), in vacuum (b), 1.0 wt% Ag/Ga_2O_3 heated at 673 K in air (c), in vacuum (d) and an Ag foil.

Figure 6. Ag L_3-edge XANES spectra of 0.1 wt% Ag/Ga_2O_3 heated in vacuum at 673 K (a), 1.0 wt% Ag/Ga_2O_3 heated in vacuum at 673 K (b) and an Ag foil. The spectra of Ag/Ga_2O_3 samples exhibit reduced intensity just above the edge relative to that of an Ag foil.

Figure 7. O K-edge XANES spectra of a bare Ga_2O_3 (a), 0.1 wt% Ag/Ga_2O_3 (b), 0.2 wt% Ag/Ga_2O_3 (c), 0.5 wt% Ag/Ga_2O_3 (d) and 1.0 wt% Ag/Ga_2O_3 (e).

Figure 8. Difference FT-IR spectra of the adsorbed species after the introduction of 45 Torr of CO_2 on a bare Ga_2O_3 (a), 0.1 wt% Ag/Ga_2O_3 (b), 0.2 wt% Ag/Ga_2O_3 (c), 0.5 wt% Ag/Ga_2O_3 (d) and 1.0 wt% Ag/Ga_2O_3 (e).

Figure 9. Difference FT-IR spectra of the adsorbed species after introduction of CO_2, followed by evacuation and photoirradiation for 1 h on a bare Ga_2O_3 (a), 0.1 wt% Ag/Ga_2O_3 (b), 0.2 wt% Ag/Ga_2O_3 (c), 0.5 wt% Ag/Ga_2O_3 (d) and 1.0 wt% Ag/Ga_2O_3 (e).

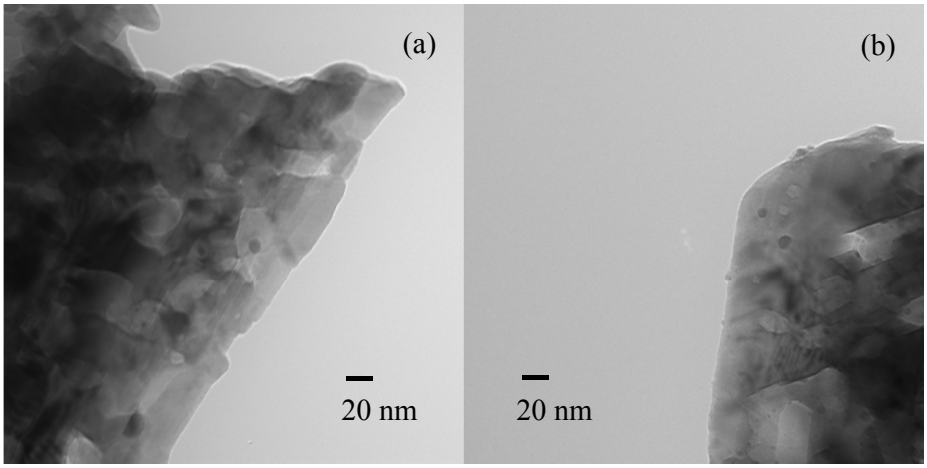

Figure 1. TEM images of 0.1 wt% Ag/Ga_2O_3 (a) and 1.0 wt% Ag/Ga_2O_3 (b).

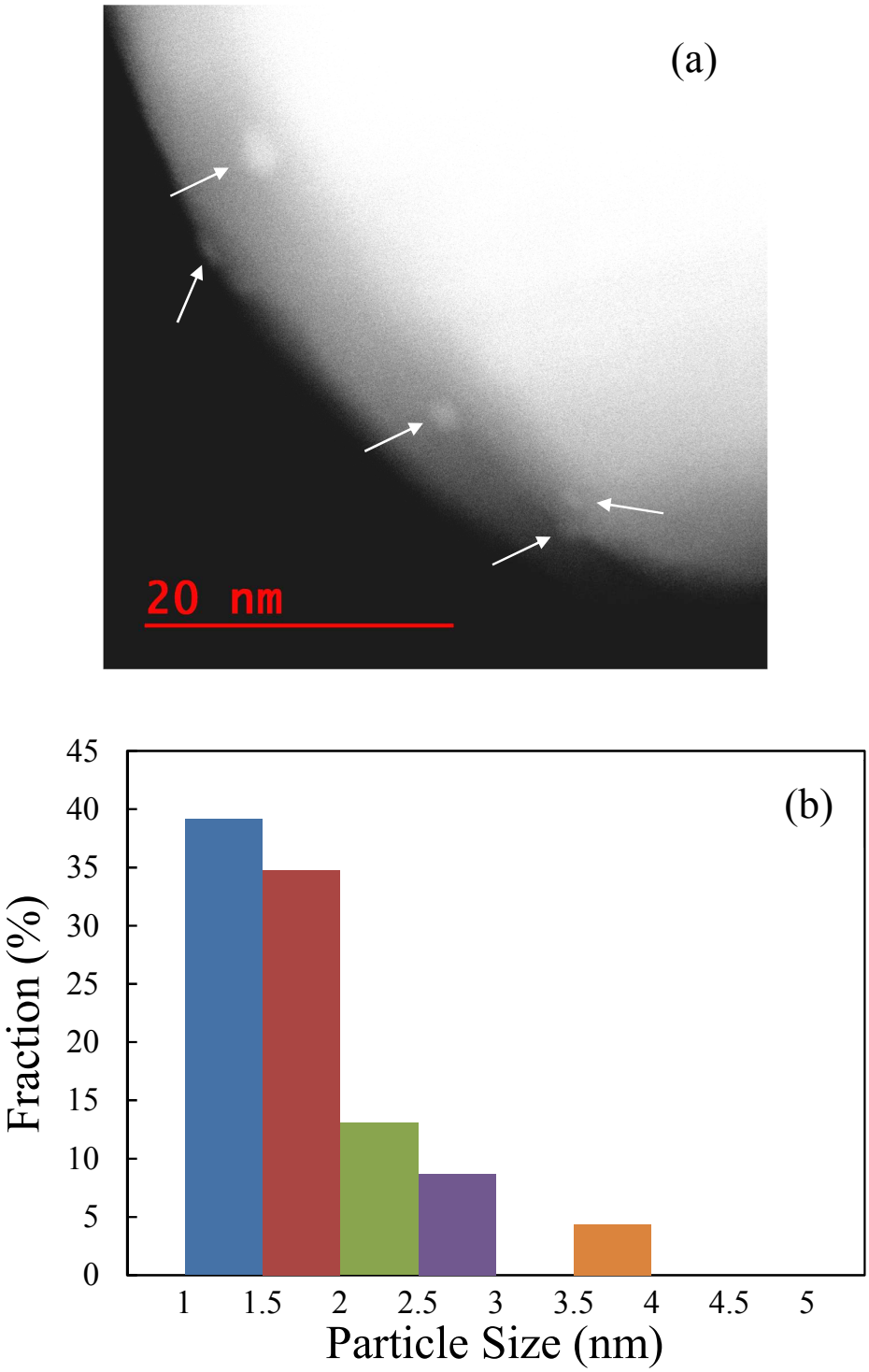

Figure 2. HAADF-STEM image of 0.1 wt% Ag/Ga_2O_3 (a) and the size distribution of Ag particles (b).

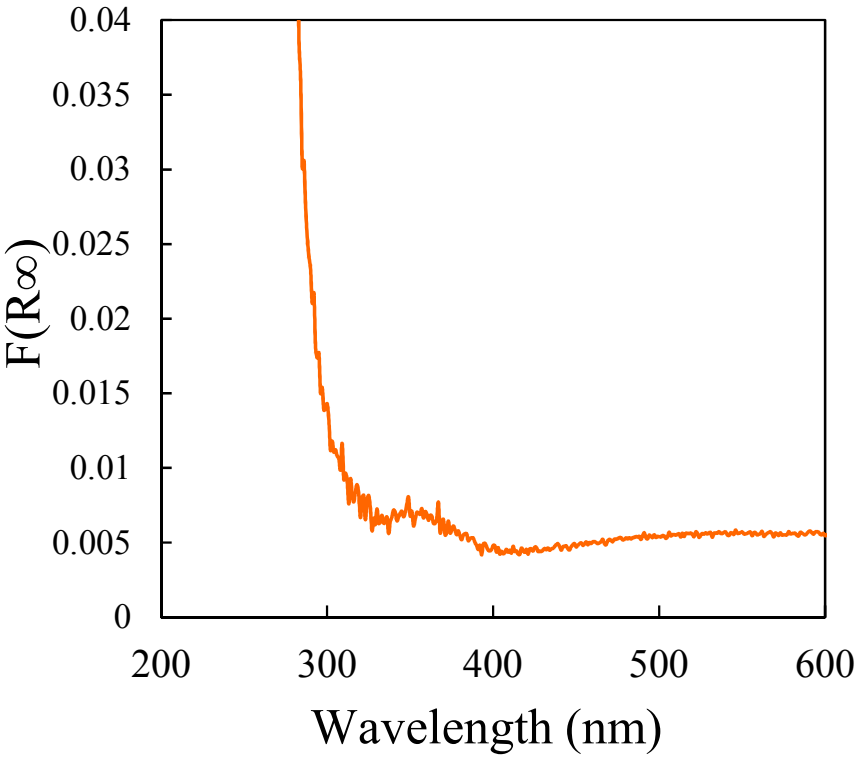

Figure 3. Diffuse reflectance UV-Vis absorption spectrum of 0.1 wt% Ag/Ga_2O_3.

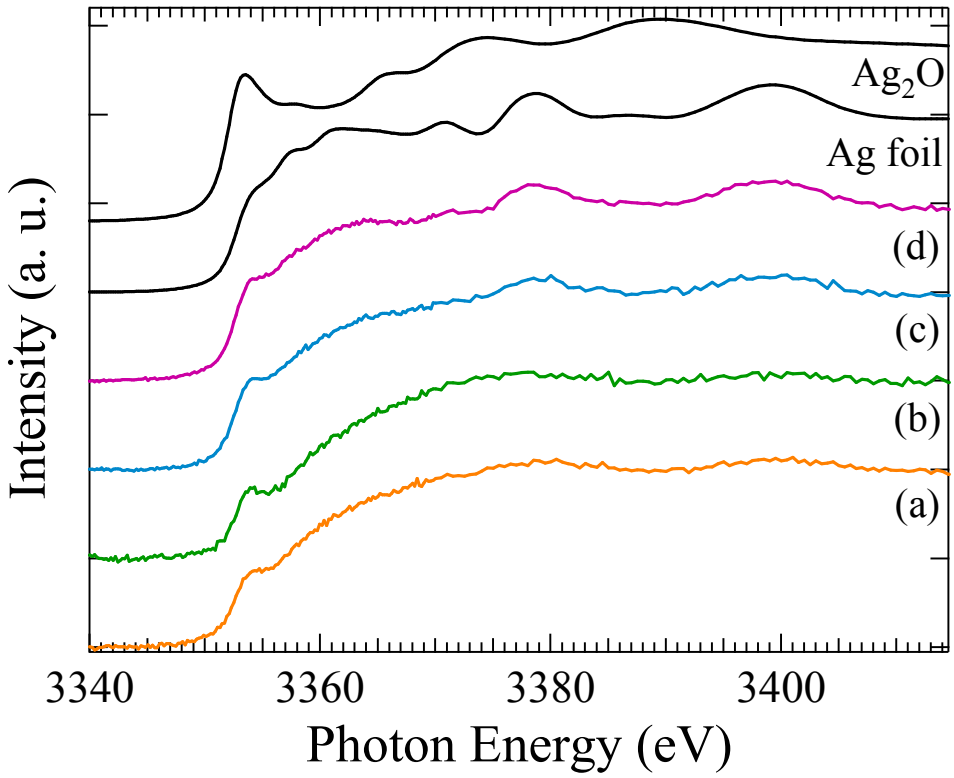

Figure 4. Ag L_3-edge XANES spectra of 0.1 wt% Ag/Ga_2O_3 (a), 0.2 wt% Ag/Ga_2O_3 (b), 0.5 wt% Ag/Ga_2O_3 (c), 1.0 wt% Ag/Ga_2O_3 (d) and Ag references.

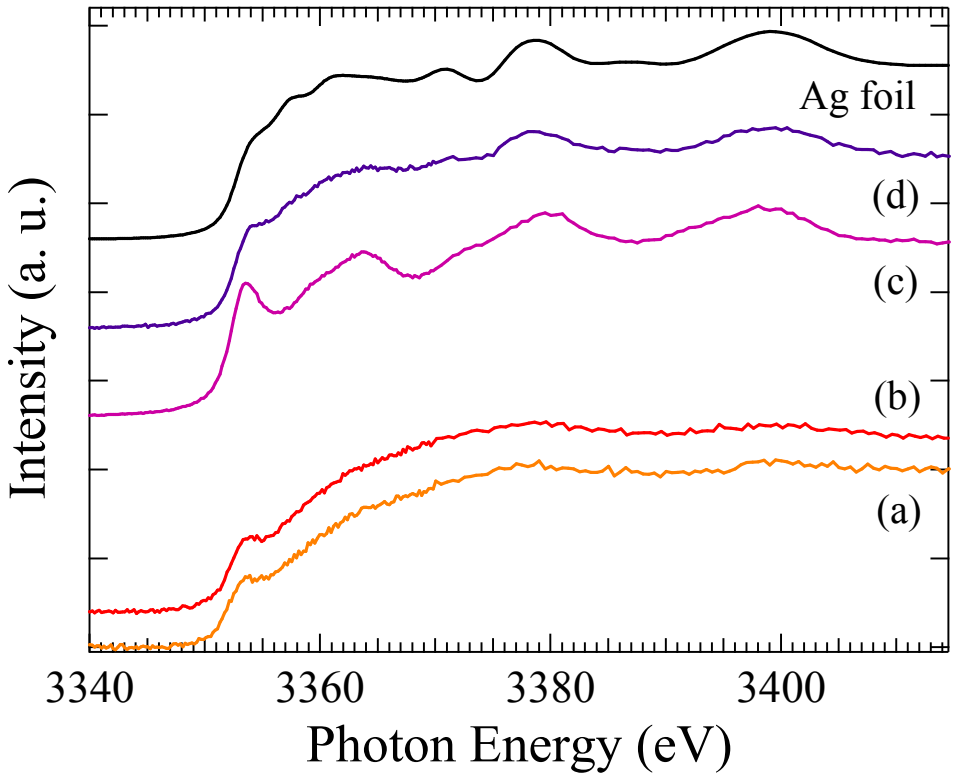

Figure 5. Ag L_3-edge XANES spectra of 0.1 wt% Ag/Ga_2O_3 heated at 673 K in air (a), in vacuum (b), 1.0 wt% Ag/Ga_2O_3 heated at 673 K in air (c), in vacuum (d) and an Ag foil.

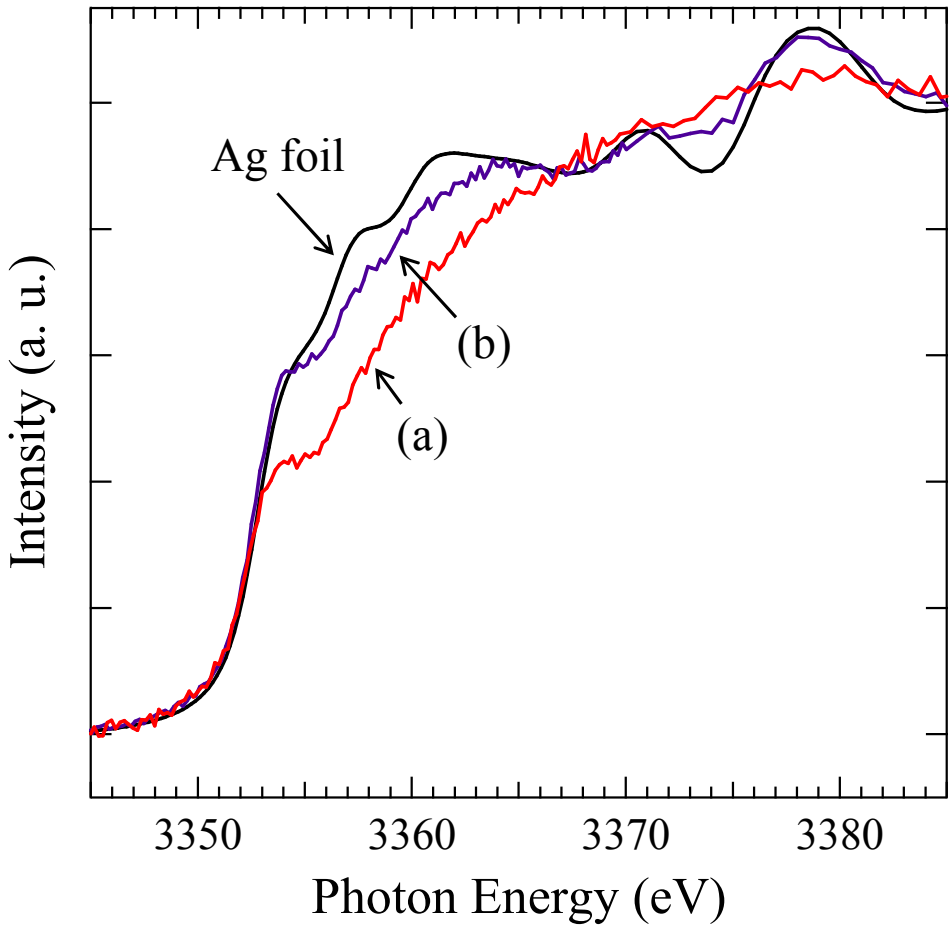

Figure 6. Ag L_3-edge XANES spectra of 0.1 wt% Ag/Ga_2O_3 heated in vacuum at 673 K (a), 1.0 wt% Ag/Ga_2O_3 heated in vacuum at 673 K (b) and an Ag foil. The spectra of Ag/Ga_2O_3 samples exhibit reduced intensity just above the edge relative to that of an Ag foil.

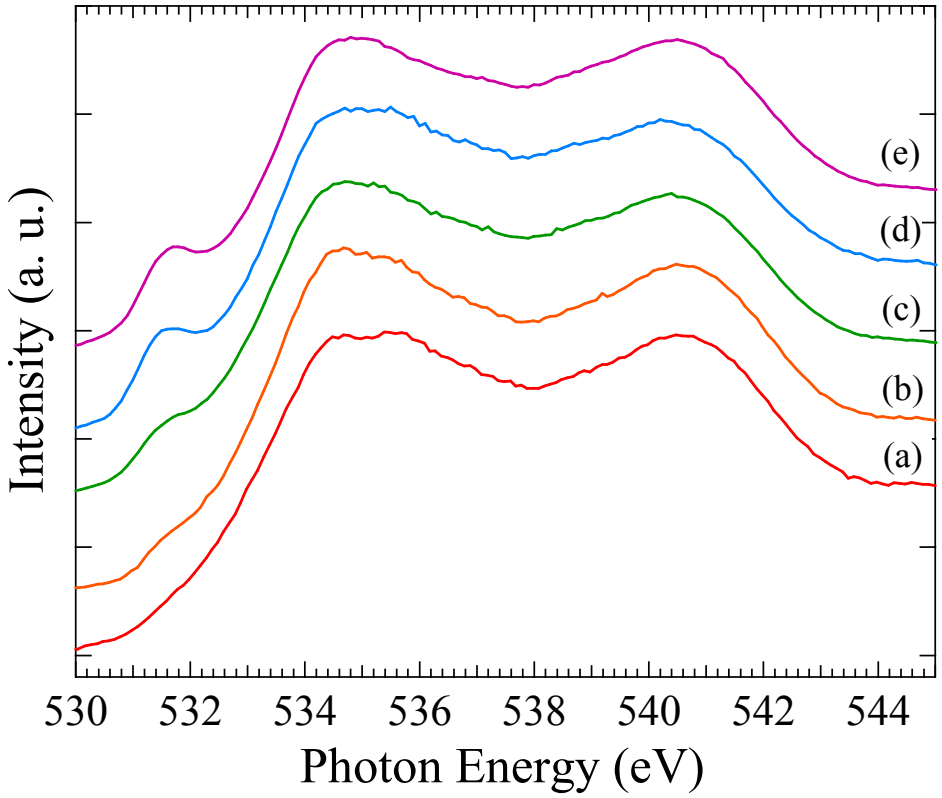

Figure 7. O K-edge XANES spectra of a bare Ga_2O_3 (a), 0.1 wt% Ag/Ga_2O_3 (b), 0.2 wt% Ag/Ga_2O_3 (c), 0.5 wt% Ag/Ga_2O_3 (d) and 1.0 wt% Ag/Ga_2O_3 (e).

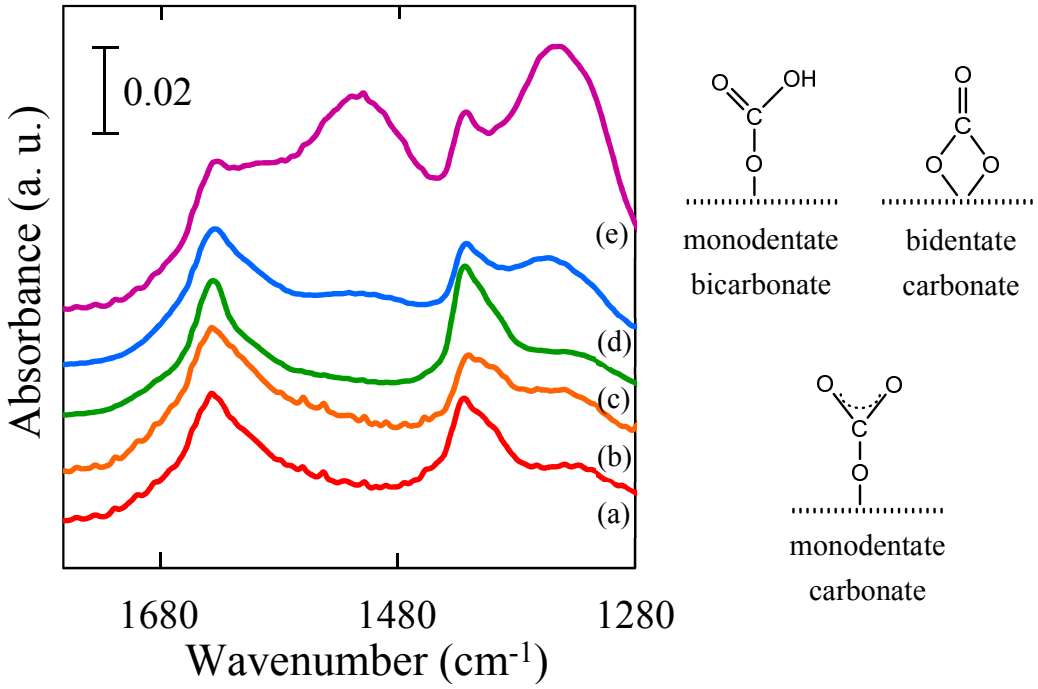

Figure 8. Difference FT-IR spectra of the adsorbed species after the introduction of 45 Torr of CO_2 on a bare Ga_2O_3 (a), 0.1 wt% Ag/Ga_2O_3 (b), 0.2 wt% Ag/Ga_2O_3 (c), 0.5 wt% Ag/Ga_2O_3 (d) and 1.0 wt% Ag/Ga_2O_3 (e).

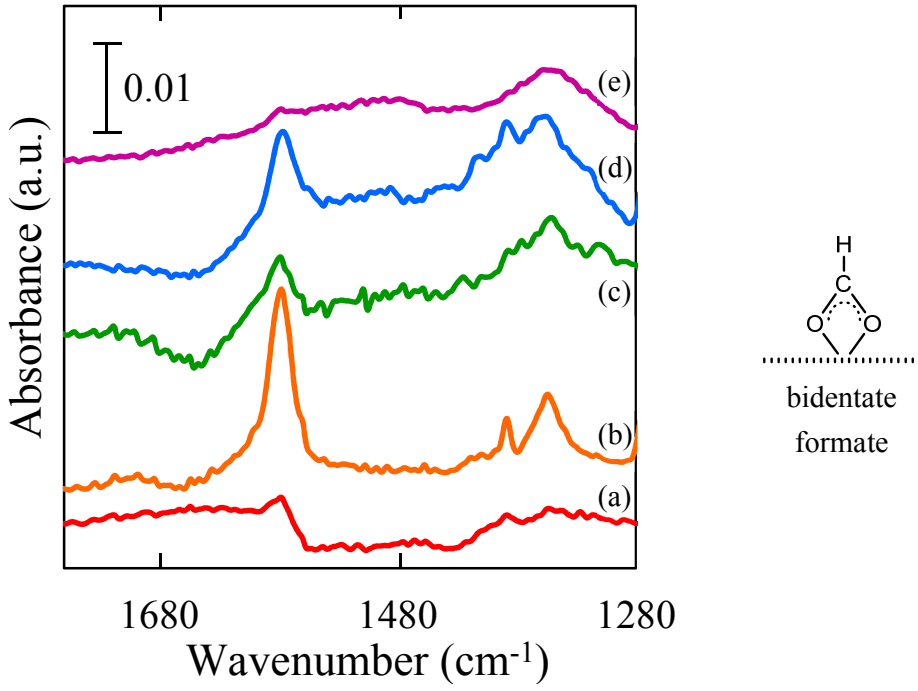

Figure 9. Difference FT-IR spectra of the adsorbed species after introduction of CO_2, followed by evacuation and photoirradiation for 1 h on a bare Ga_2O_3 (a), 0.1 wt% Ag/Ga_2O_3 (b), 0.2 wt% Ag/Ga_2O_3 (c), 0.5 wt% Ag/Ga_2O_3 (d) and 1.0 wt% Ag/Ga_2O_3 (e).